Numerical Investigation of the Effect of Moisture on Buoyancy-driven Low Turbulence Flow in an Enclosed Cavity

Dr Draco Iyi[1*], Dr Reaz Hasan[2]

[1*]Department of Mechanical Engineering, School of Engineering
Robert Gordon University Aberdeen, AB10 7GJ, United Kingdom
Phone: +44 (0) 1224 262412; Email: d.iyi@rgu.ac.uk

[2]School of Engineering and the Built Environment,
Birmingham City University, Birmingham B4 7AP

Abstract

This paper reports a numerical investigation of low turbulence buoyancy-driven flow of moist air and heat transfer inside a rectangular cavity with differentially heated vertical walls. The purpose is to provide a detailed technical knowledge on the effect of moisture transfer in enclosures where humidity plays an important role through effective prevention or mitigation against the risk of condensation. Moisture management in an enclosed environment at the design threshold is important since condensation can cause material damage (delamination, circuit oxidation and condensation in electronic enclosures) and optimise energy use in buildings. The accuracy of the numerical methodology was also scrutinised by conducting a rigorous validation study of benchmark experimental data for the average Nusselt number for similar buoyancy driven cavity flow.

The variations of the flow, temperature and moisture fields inside the cavity has been analysed together with the heat transfer coefficients for a range of mass fraction of water vapour and the temperature gradients between the vertical walls of the cavity. The results of this investigation showed that during the natural convection process, the charge in moisture content in the moist air has a significant influence on the flow and temperature fields inside the enclosure and the variation of the vertical wall temperature gradients have also shown to affect the moisture concentration inside the cavity. The percentage change in the average heat transfer varied significantly depending on the mass fraction of moisture in the moist air and the temperature gradient between the vertical walls. The result also shows a 3.5% increase in the average heat transfer for every 0.02 kg/kg increment in the mass fraction of water vapour.

.

Keywords: *Natural convection, Buoyancy-driven flow, Moisture transport, Heat transfer, Computational Fluid Dynamics.*

Nomenclature

C_p	specific heat at constant pressure, J/(kg-K)
C_μ	empirical constant in turbulence models
g	gravitational acceleration, m/s^2
H	height of the cavity, m
J_i	mass flux of species (J/m^2 -s)
k	turbulent kinetic energy, m^2/s^2
$\overline{k}$	average thermal conductivity, W/(m-K)
L	width of the cavity, m
Nu	local Nusselt number
$\overline{Nu}$	average Nusselt number
$\% \Delta \overline{Nu}$	percentage change in average Nusselt number
m_i	local mass fraction of vapour
Q	local heat flux, W/m^2
$\overline{Q}$	integral average heat flux, W/m^2
Ra_H	Rayleigh number based on height
S	source terms
T	temperature (K, $^\circ$C)
ΔT	local temperature difference
T_c	cold wall temperature (^{o}C)
T_h	hot wall temperature ($^\circ$C)
v_x	fluid velocity component in x-direction, m/s
v_y	fluid velocity component in y-direction, m/s
x, y, z	cartesian coordinates
y^+	non-dimensional wall distance

Greek symbols

α	thermal diffusivity, m^2/s
β	thermal expansion coefficient, I/K
ε	turbulent dissipation rate, m^2/s^2; Emissivity
ρ	fluid density, kg/m^3
σ	Stefan-Boltzmann constant, (5.6721×10^{-8} W/m^2-K^4)
μ	dynamics viscosity kg/m-s
v	kinematic viscosity, m^2/s

1.0. **Introduction**

Natural convection driven flow in enclosures has been the subject of extensive research activity for the last four decades because of its relevance in many practical applications [1-4]. The interest seems to be ongoing because more challenging situations are emerging with time and a considerable number of studies have been conducted of which reviews are available [5-7].

An idealised configuration of natural convection set up which has also attracted most attention is the case of a rectangular cavity with opposing vertical walls that are heated differentially [8-10] of which experimental data for the flow velocities, turbulence quantities and wall heat transfer coefficients are available [8, 11]. The temperature difference between the vertical walls results in density difference, and if the buoyancy forces associated with the density difference are sufficient to overcome the viscous forces, a natural convection characterised by the formation of a slow moving vortex is developed. Natural convection flows in an indoor environment are mostly associated with coupled heat and moist air transport processes [12]. Therefore, analysis of natural convection in an indoor space demands a detailed representation of the air-moisture and thermal fields established inside the enclosed space.

A recent shift in the study of natural convection driven flow in a differentially heated cavity is the examination of coupled heat and mass transfer [13-15]. Amongst many other factors that influence the buoyancy-driven flow phenomenon, such as the Rayleigh number, the nature of fluid, etc., is the presence of water vapour in the air. The amount of water vapour in the air is an important factor that influences indoor air quality, energy consumption in buildings and the durability of building materials [16-17].Condensation on material surface is usually perceived as a risk in the storage of artefacts/cultural heritage objects and in a built environment since it can cause material damage, mechanical stress due to hygroscopic swelling, oxidation of metals and delamination.

Design for indoor humidity control is important for the moderation and control of moisture transport in applications involving cooling or heating processes and in the cavity of building walls [18-20]. Therefore, it is important to evaluate and quantify the influence of moisture on natural convection flow and heat transfer in order to enhance the performance of such applications. For example, storage facilities involving historic building materials and artefacts have a certain recommended operational humidity threshold. For such facility, humidity below the recommended level could result in induced stress and strain [21-24], and high humidity level could result in a significant damage of the materials. Also, the risk of too low or too high humidity in an indoor environment of the human occupant, building materials, storage and drying operations has also been given serious considerations [25-28].

There are few studies available in literature on the effect of moisture on buoyancy–driven natural convection flow and heat transfer characteristics between vertical plates and enclosed space with temperature gradient between the vertical walls [15, 29-30]. Yan and Lin [31] investigated the effects of latent heat transfer in association with water vapour evaporation from the surface of a wet channel wall on the natural convection heat transfer. Their results showed that a significant improvement in heat transfer was due to the exchange of latent heat of vaporisation and that the Grashof number is a function of the relative humidity. Sun et al. [15], have numerically investigated the coupled natural convection to wall condensation/evaporation in a two-dimensional cavity filled with quiescent humid air subjected to time-dependent wall uniform temperatures. They observed that condensation/evaporation occurred on the surface of all four walls during the natural convection process. Their results showed that the introduction of water vapour changes the flow pattern especially near the wall surfaces when compared with a similar cavity filled with dry air only.

Experimental study conducted by Lin et al. [32], used herringbone wavy wet wall fin geometry to show that the heat transfer does depend on the level of water vapour present in such an enclosure. Laguerre et al. [29], investigated the flow and heat

transfer characteristic in a refrigerating cavity with and without the presence of moisture. Their experimental test rig was similar to that of a typical domestic refrigerator, but with a heated water vat at the bottom. Their result showed that water evaporation significantly influences the air velocity and temperature fields. Similar flow behaviours were also observed in the experimental work reported by Laguerre et al. [14], using a cavity partially filled with isolated cylindrical pipes.

Despite various researches acknowledged that moisture in air influences the natural convection flow characteristics, however, none of the reported work explicitly specifies such effects. This paper provides further understanding of coupled flow, heat and moisture transport due to natural convection in a differentially heated rectangular cavity and also provides an explicit analysis of the effect of moisture concentration in moist air on the buoyancy-driven natural convection heat transfer coefficient in the enclosure. A range of mass fraction of water vapour and wall thermal conditions was used for the study in order to provide some quantitative and qualitative flow and heat transfer behaviours due to the changes in the vertical wall temperature gradients and moisture concentration in moist air. The study can be used as a guide during the design phase of relevant system to detect conditions with potential risk of condensation even before the phase change occurs. It will assist to identify sensitive areas to lower moisture content or increase temperature and also to avoid condensation by optimizing the design of such enclosed system so that the relative humidity remains below a given threshold.

2.0. **Problem Description**

The geometrical configuration used in this study is similar to the rectangular cavity used by Ampofo and Karayiannis [8]. The rectangular cavity is 1.5 m in depth (Z) and 0.75 m in length (L) and height (H) which resulted in a two-dimensional flow in the mid-plane (=Z/2) of the cavity as shown in Figure 1. To investigate the influence of temperature on moisture concentration inside the enclosure, a range of mass fraction of water vapour was used and the vertical wall temperature gradient ($\Delta T = T_h - T_c$) varied from 20 to 60 °C with an increment of 10 °C for each value of mass fraction of vapour. The effect of moisture concentration in moist air was investigated using a fixed vertical wall temperature gradient but with a varying mass fraction of the water vapour from 0 to 0.12 kg/kg with an increment of 0.005 kg/kg.

The base case is a cavity filled with dry-air only with the water vapour mass fraction of 0 kg/kg and was also used to validate our numerical approach. The mass fraction of water vapour in moist air is the mass of water vapour in the moist air to the mass of dry air. The mass fraction of water vapour of 0 kg/kg was imposed on the cold wall (m_c), while that on the hot wall (m_h) was varied accordingly. For the validation study, the top and bottom walls were fixed at zero diffusive flux with the experimental temperature by Ampofo and Karayiannis [8] used as the thermal boundary condition, while an adiabatic thermal condition was specified for enclosures containing air and water vapour mixture.

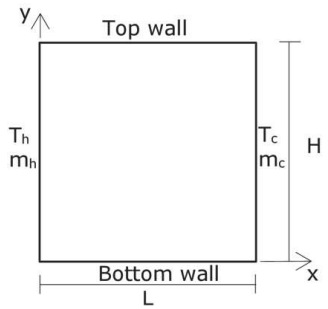

Figure 1: schematic of the enclosure and the boundary conditions

The natural convection heat transfer from hot to cold wall is characterised by the formation of a slow moving vortex. Fluid flow up along the hot vertical wall by absorbing heat from the 'source', and then it flows downward along the cold wall gradually losing the heat to the cold surface which may be termed as the 'sink'. Depending on the Rayleigh number shown in Eq. (1), the flow can be turbulent or laminar and for Rayleigh number greater than $10^9$the flow is found to be dominated by turbulence near the walls [33-34].

$$Ra = \frac{g\beta(T_h - T_c)L^3}{\nu\alpha} \quad (1)$$

Where, β is the coefficient of thermal expansion, ν and α represent the kinematic viscosity and the thermal diffusivity of the fluid respectively. The Rayleigh number of the cases presented in this paper ranges from 7.89×10^8 to2.37×10^9.

3.0. **Numerical method**

Integrated numerical simulation of the coupled flow, heat and vapour transport inside the cavity with vertical wall temperature differential was performed using the commercial Computational Fluid Dynamics (CFD) tool called ANSYS Fluent [35]. The CFD tool has been used widely to explore various practical flows involving natural convection phenomenon [36-37]. The methodology involves the iterative solution of Navier-Stokes equations along with continuity and energy equation using the SIMPLE algorithm on collocated variables. With the SIMPLE scheme, the velocity correction is solved explicitly while the discretized momentum equation and the pressure correction equation are solved implicitly. The SIMPLE algorithm is described by Patankar [38], Ferzier and Peri [39] and Qi-Hong and Guang-Fa [40]. The steady state flow conservation equations for continuity, velocity components and temperature are shown in Eq.(2) to Eq.(5).

Continuity equation

$$\frac{\partial(\rho u)}{\partial x} + \frac{\partial(\rho v)}{\partial y} = 0 \quad (2)$$

Momentum equation in y-direction

$$\frac{\partial(\rho v u)}{\partial x} + \frac{\partial(\rho v v)}{\partial y} = -\frac{\partial p}{\partial y} + \frac{\partial}{\partial x}\left[\mu_{eff}\left(\frac{\partial v}{\partial x} + \frac{\partial u}{\partial y}\right)\right] + \frac{\partial}{\partial y}\left[2\mu_{eff}\frac{\partial v}{\partial y}\right] + \rho\beta g(T - T_o) \quad (3)$$

Momentum equation in x-direction

$$\frac{\partial(\rho u u)}{\partial x} + \frac{\partial(\rho v u)}{\partial y} = -\frac{\partial p}{\partial x} + \frac{\partial}{\partial x}\left[2\mu_{eff}\frac{\partial u}{\partial x}\right] + \frac{\partial}{\partial y}\left[\mu_{eff}\left(\frac{\partial u}{\partial y} + \frac{\partial v}{\partial x}\right)\right] \quad (4)$$

General transported fluid scalar, $\phi\ (i.e., T, k, \varepsilon)$

$$\frac{\partial}{\partial x}(\rho u \phi) + \frac{\partial}{\partial y}(\rho v \phi) = \frac{\partial}{\partial x}\left(\Gamma_\phi \frac{\partial \phi}{\partial x}\right) + \frac{\partial}{\partial y}\left(\Gamma_\phi \frac{\partial \phi}{\partial y}\right) + S_\phi \quad (5)$$

Where, ϕ represents the concentration of the transported quantity for the momentum, scalar mass and the energy conservation equations and Γ_ϕ is the exchange coefficient for ϕ .

From a numerical analysis point of view, the accuracy of computations is affected by several factors; such as the choice of viscous models, grids, discretization schemes and convergence, which has been a concern for numerical scientists [38-40]. For greater accuracy, these uncertainties that may influence the flow physics were carefully taken into account in the numerical modelling process.

It is worthwhile to note that the process of computing a steady-state solution using very fine mesh has been quite challenging because of the oscillations associated with higher-order discretization schemes. As a result, a number of steps were taken to achieve a steady-state solution. Initially, low value of Rayleigh number was adopted for the solution using an incompressible unsteady solver with the first-order scheme for convection terms. The resulting data files for the three cases were then used as an initial guess for the higher Rayleigh number simulation using the higher-order discretization schemes. This method helped to create a more realistic initial field for low-Reynolds number *k-ε* runs. For the discretization of convection schemes, second order schemes have been used in the convection terms of momentum, energy and water vapour except for the Pressure term where PRESTO was used.

3.1. Turbulence modelling

Turbulent fluxes of momentum and heat were modelled by low-Reynolds number *k*-epsilon Eddy Viscosity Model of Launder-Sharma [41] with the inclusion of the buoyancy terms in the energy equation. More details of buoyancy model may be found in Henkes and Hoogendoorn [42]. The performance of Launder-Sharma model has been scrutinized and evaluated by various researchers and present generally better performance for low turbulence natural convection flow [43-47]. Unlike the high Reynolds number *k-ε* model, the transport equations in the low-Reynolds number model can be integrated up to the wall. Based on Bousinesq approximation, the Reynolds stress is related to the local velocity gradients by an eddy viscosity v_t. The turbulent scalar quantities (*k* and *ε*) used to calculate the eddy viscosity are determined from the transport equations of turbulent kinetic energy and its dissipation, both represented in Eq. (6) and Eq. (7) respectively.

$$\frac{\partial(\rho k)}{\partial t}+\frac{\partial(\rho U_j k)}{\partial x_j}=\frac{\partial}{\partial x_j}\left[\left(\mu+\frac{\mu_t}{\sigma_k}\right)\frac{\partial k}{\partial x_j}\right]+P_k+G_k+\rho\varepsilon+D \tag{6}$$

$$\frac{\partial(\rho\varepsilon)}{\partial t}+\frac{\partial(\rho U_j \varepsilon)}{\partial x_j}=\frac{\partial}{\partial x_j}\left[\left(\mu+\frac{\mu_t}{\sigma_\varepsilon}\right)\frac{\partial \varepsilon}{\partial x_j}\right]+C_{\varepsilon 1}f_1\frac{\varepsilon}{k}\left(P_k+G_k\right)-C_{\varepsilon 2}f_2\frac{\varepsilon^2}{k}+E \tag{7}$$

Where the eddy viscosity $\mu_t=\rho C_\mu f_\mu\left(k^2/\varepsilon\right)$, and the numerical values assigned to the constant are: $C_\mu=0.09;\quad C_1=1.44;\quad C_2=1.92;\quad \sigma_k=1.0$ and $\sigma_\varepsilon=1.3$

P_k is the generation of turbulence kinetic energy due to the mean velocity gradients and the generation of turbulence kinetic energy due to buoyancy is $G_k=-\beta g\left(\mu_t/\sigma_{t,\varphi}\right)\left(\partial\varphi/\partial y\right)$.

The expressions for the terms $D=2\nu\left(\partial\sqrt{k}/\partial y\right)^2$ and $E=2\mu\frac{\mu_t}{\rho}\left(\partial^2 U/\partial y^2\right)^2$

These terms are needed to balance the molecular diffusion of *k* in order to satisfy the transport equation in the near wall region. At low Reynolds numbers, the damping functions f_μ and f_2 become dependent upon the value of the turbulence Reynolds number Re_t. Where $Re_t=\rho k^2/\mu\varepsilon$,

$f_\mu=exp\left(-3.4/\left(1+\mathrm{Re}_T/50\right)^2\right);\quad f_1=1.0\quad and\quad f_2=1-0.3exp\left(-Re_T^2\right)$

The main implication of the low-Reynolds number k-ε model functions $\left(f_{\mu}, f_1 \text{ and } f_2\right)$ is to modify the models constants C_{μ}, C_1 and C_2 to account for low Reynolds number effects.

3.2. Radiation modelling

The Discrete Ordinate Method (DOM) [48-49] has been used to simulate the radiative heat transfer between all wall surfaces and the fluid for both the humidified and un-humidified cases. The DOM has been chosen due to its proven superiority in predicting radiative heat transfer involving a participating medium and surface-to-surface radiation as reported by Versteeg and Malalasekera[50] and Iyi et al. [51]. The humid air was treated as absorbing-emitting and non-scattering gray medium. The DOM solves the radiative transfer equation for a finite number of discrete solid angles and spans the entire range of optical thickness. The model considers the radiative transfer equation in the direction $\vec{s}$ and position vector $\vec{r}$ as a field equation shown in Eq. (8) [50].

$$\nabla.\left(I_{\lambda}\left(\vec{r},\vec{s}\right)\vec{s}\right)+\left(a_{\lambda}+a_{s}\right)I_{\lambda}\left(\vec{r},\vec{s}\right)=a_{\lambda}n^{2}\frac{\sigma T^{4}}{\pi}+\frac{\sigma_{s}}{4\pi}\int_{0}^{4\pi}I_{\lambda}\left(\vec{r}.\vec{s}\,'\right)\varphi\left(\vec{s}.\vec{s}\,'\right)d\Omega' \qquad (8)$$

Where $\vec{s}$ is the direction vector, $\vec{s}'$ is the scattering direction vector, $\vec{r}$ is the position vector, I_{λ} is the radiation intensity of the wavelength, φ is the phase function, Ω' is the solid angle in radian and σ is the Stefan-Boltzmann constant.

3.3. Moisture transport modelling

The fluid used was computed as a binary mixture of water vapour and air. The vapour-air interaction has been modelled by adding to the basic flow equation a convection-diffusion conservation equation of vapour mass fractions. The species transport model considered the vapour as a scalar transport by the airflow and at the same time the water vapour influence the airflow governing equations. The vapour content present in the moist air was defined by the local vapour mass fraction $m_{i'}$ which is defined as the ratio of the mass of water vapour to the mass of the total mixture. In the presence of a dynamic field characterised by a velocity u_i the conservation equations [35] in tensor notation is shown in Eq.(9), and represents the convection-diffusion relation;

$$\frac{\partial}{\partial x_i}\left(\rho u_i m_{i'}\right)+\frac{\partial}{\partial x_i}J_{i',i}=S_{i'} \qquad (9)$$

The convective term is the first term on the left-hand side and the second term represent the diffusion flux, while the last term $S_{i'}$ is the rate of species creation in addition to any user-defined sources. The diffusion flux represented in Eq.(10)accounts for the diffusion due to concentration gradients and any additional mass diffusion caused by turbulence.

$$J_{i'}=-\left(\rho D_{i',m}+\frac{\mu_t}{Sc_t}\right)\frac{\partial m_i}{\partial x_i}-\frac{D_{T,i}}{T}\frac{\partial T}{\partial x_i} \qquad (10)$$

Where, Sc_t is the turbulent Schmidt number which accounts for the turbulent diffusivity, $D_{i',m}$ is the mass diffusion coefficient of the water in the humid air and $D_{T,i}$ represents the thermal diffusion coefficient. The convection-diffusion equation [Eq. (9)] is added to the flow model to take into account the interaction of water vapour mass fraction in the domain.

3.4. *Boundary conditions and material properties*

A validation study was conducted by setting the temperature of the hot and cold wall at $50\ ^{o}C$ and $40\ ^{o}C$ respectively resulting in Rayleigh number of 1.58×10^{9}. The horizontal walls were set as conducting walls and using a best-fit polynomial adopted from the dimensionless temperature profile $[T = T_c - (T - T_c)]$ as a function of the dimensionless distance (x/L)along the top and bottom walls based on the experimental benchmark data by Ampofo and Karayiannis [8] shown in Figure 2. This represents the most realistic boundary conditions at the top and bottom horizontal walls since the setup was used for the validation. The coefficients for the best-fit polynomial $T^{*} = a(x/L)^4 + b(x/L)^3 + c(x/L)^2 + d(x/L) + 1$ are displayed in Table 1. The temperature profiles were coded in C++ programming language and incorporated into ANSYS-FLUENT through the User-Defined-Function with zero diffusive flux imposed on all walls.

Table 1: Coefficients for the polynomial

Walls	*a*	*b*	*c*	*d*
Top	-2.458	1.686	1.211	-1.440
Bottom	2.458	-8.146	8.477	-3.789

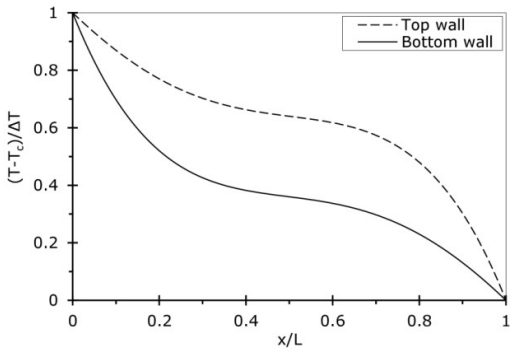

Figure 2: temperature profiles for top and bottom wall

In order to investigate the influence of moisture transport on the flow and heat transfer, isothermal temperature boundary conditions were assumed for both vertical walls and zero heat flux was imposed on the top and bottom walls. A reference case was considered for all temperature range used in the study in order to evaluate the effect of moisture on the flow and heat transfer. Fixed temperature of 10 ^{o}C was imposed on the cold wall; while the temperature at the hot wall was varied from 30 ^{o}C by an increment of 10 ^{o}C resulting in Rayleigh number ranges from 7.89×10^{8} to 2.37×10^{9}. The mass fraction of water vapour was varied from 0 kg/kg to 0.12 kg/kg with an increment of 0.005 kg/kg. Instantaneous vapour diffusion was assumed at the hot and the vapour concentration in the enclosed cavity was modelled using the species transport model. Both the dry-air and air-vapour mixture cases were modelled as a participating medium using the DOM with 0.9 specified for emissivity on all the walls.

The thermos-physical properties of each consistent specie in the fluid mixture was evaluated using the temperature average between the vertical walls, while the combined mixture properties were defined as follows; incompressible ideal gas was specified for the density, mass weighted mixing law for the thermal conductivity and viscosity, kinetic theory was selected for the mass diffusivity and thermal diffusion coefficient. The specific heat of the mixture was defined as the mass fraction average of the air and vapour heat capacities. The second order upwind discretization scheme was used for the convection terms of each governing equation, except for the pressure term were the PRESTO scheme was used.

4.0. **Grid Sensitivity Analysis and Validation**

At the very outset of this study, we decided to scrutinise grid sensitivity effect and the results for the near-wall y-plus (y^+) distributions along the horizontal and vertical walls are presented in Figure 3. The y^+ value is a non-dimensional distance from the wall to the first mesh node. Since natural convection are wall-bounded flows, therefore, accurate presentation of the flow in the near-wall region determines the successful prediction of flow and heat transfer and a y-plus value of about 1 are desirable for near-wall modelling. A mesh density of 200 × 200 with grids clustering near the walls and y-plus values well below 1 was adopted for all simulations reported in this paper. The results of the validation study are shown in Figure 4 (a-d). The temperature profile at mid-width and the velocity profile near the hot wall compared favourably well with the experimental data of Ampofo and Karayiannis [8]. The wall heat transfer coefficient (Nusselt number) also shows a favourable comparison with the experimental data as shown in Figure 4 (c-d).

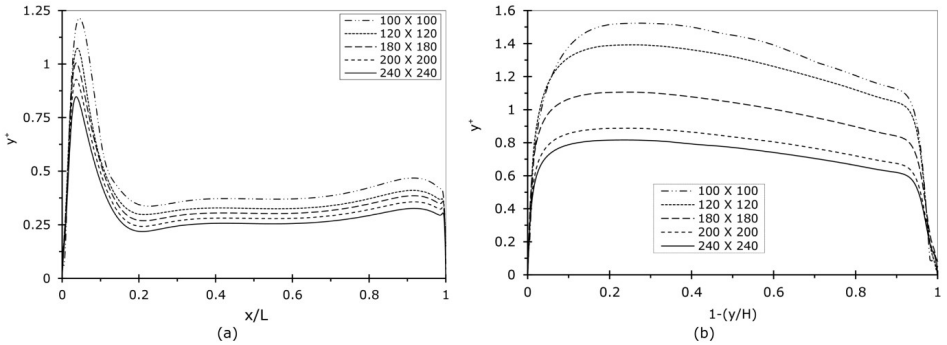

Figure 3: comparison of y-plus profile (a) top wall (b) cold wall

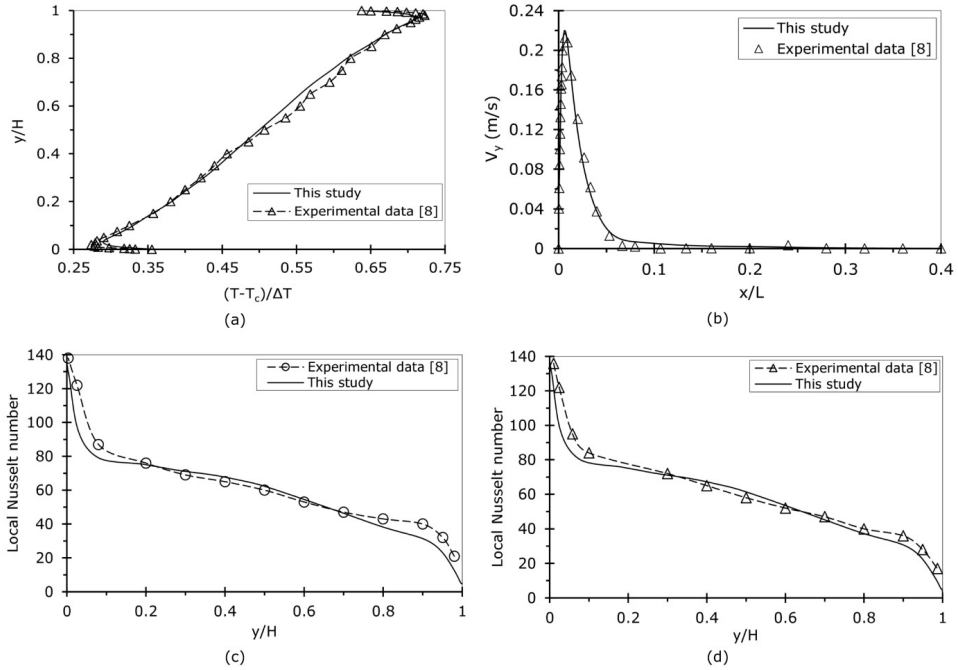

Figure 4: Comparison of numerical and experimental results (a) Temperature profile at mid-width (b) velocity profile at mid-height near hot wall (c) Cold wall local Nusselt number (d) hot wall local Nusselt number.

The average Nusselt number for the un-humidified case (m=0 kg/kg) has been compared with experimental benchmark data to Ampofo and Karayiannis [8]. The validation shows very good comparisons for all the walls with a minimum and a maximum error of about 0.8% and 3% associated with the bottom and cold wall respectively. The top and hot wall had shown about 2.5% of percentage error. The average Nusselt number comparisons are presented in Table 2.

Table 2: Comparisons of wall average Nusselt number

Un-humidified cavity (m=0)	Top wall	Bottom wall	Cold wall	Hot wall
This study	13.55	14.28	60.58	61.15
Experimental Data [8]	13.90	14.40	62.60	62.90

5.0. **Results and Discussions**

The effect of varying the mass fraction of vapour in the air-vapour mixture as a function of vertical wall temperature gradients on the behaviour of the natural convection flow and heat transfer coefficient are presented in this section. The average relative humidity inside the cavity for the various vapour mass fractions at different temperature are presented first and then followed by the flow and temperature fields. The variances of the wall heat transfer coefficient as a function of mass fraction of vapour for the various temperature gradients between the vertical walls were evaluated and presented thereafter as a local Nusselt number and percentage change in average Nusselt number.

5.1. Cavity average relative humidity

For the range of the mass fraction of water vapour used in the study, the cavity average relative humidity was evaluated and plotted for the different temperature gradients between the vertical walls as shown in Figure 5 (a). It is our intention that by quantifying the average relative humidity inside the cavity for the various mass fractions of vapour will offer a better understanding of how it influences the behaviour of the natural convection flow and heat transfer inside the cavity. The variation of cavity average relative humidity as a function of temperature gradients between the vertical walls for various mass fractions of vapour is shown in Figure 5 (b). It can be observed that the moisture content in the moist air is strongly dependent on the temperature gradient between the vertical walls. Therefore, one of the importances of modelling moisture transport in an indoor environment is to identify potential risk of condensation even before phase change occurs. This will assist in locating sensitive areas in the enclosed system where the relative humidity remains below or above a given threshold and in humidity management by moderating the moisture content or temperature in such sensitive areas to avoid condensation.

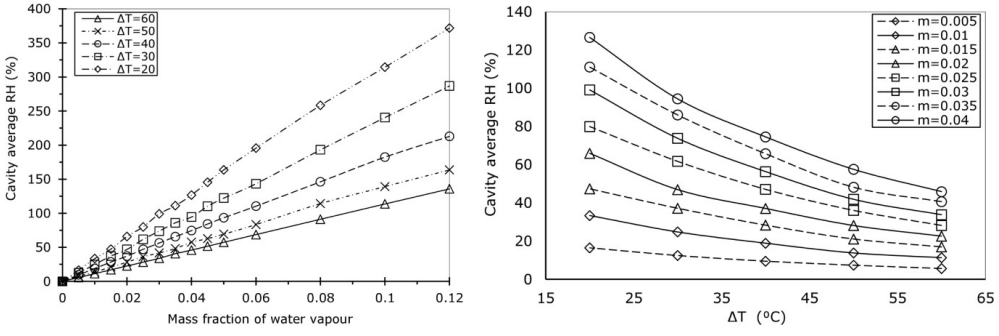

Figure 5: cavity average relative humidity as a function of (a) mass fraction of vapour (b) temperature gradients of cavity vertical walls.

5.2. *Flow and temperature fields*

It is known that temperature influences air and water vapour transport via the thermal properties and accounts for the latent heat of vaporisation. Since water vapour and dry air have different physical and thermal properties, therefore, the thermal properties of the fluid mixture are significantly dependent on the moisture content in the moist air. Therefore, the change of water vapour content in the moist air will affect the behaviour of the natural convection flow and heat transfer inside the cavity.

The comparison of temperature distribution field inside the cavity for the un-humidified case and humidified cases of mass fraction of 0.04 and 0.08 kg/kg each for two temperature gradients of 40 and 60 °C are shown in Figure 6 respectively. Temperature stratification behaviour can be observed in all the cases, but there are variations of temperature distribution inside the cavity with the various mass fractions of vapour used. Therefore, temperature distributions inside the cavity is a function of the water-vapour content in the moist-air, with significant changes near the top wall region when compared to the bottom wall region. Figure 7 shows the comparison of the moisture concentration fields of the cases involved three different vertical wall temperature gradients of 20 °C, 40 °C and 60 °C using two mass fraction of vapour of 0.002 kg/kg and 0.008 kg/kg respectively.

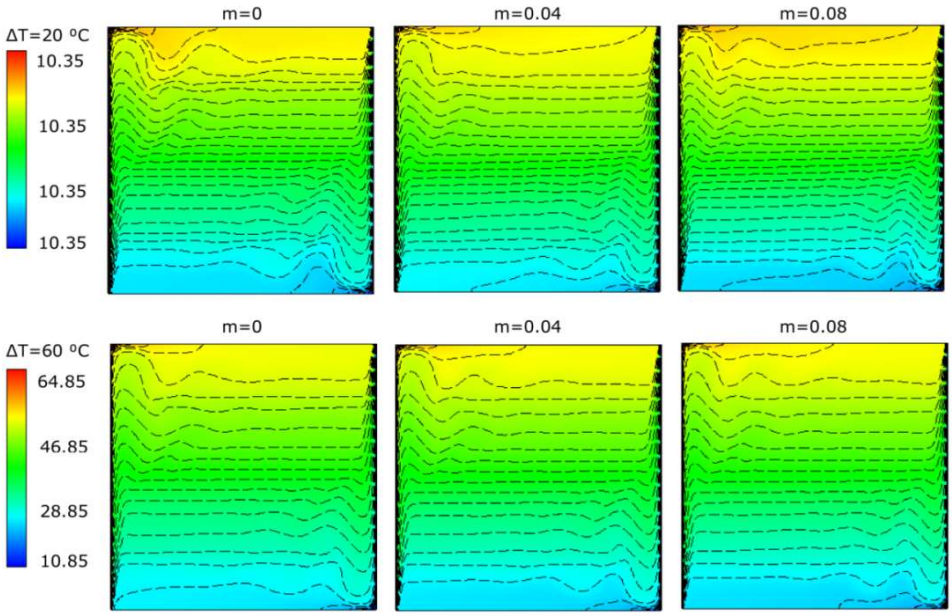

Figure 6: comparison of temperature distribution fields as a function of mass fraction of vapour for two temperature gradients of cavity vertical walls.

Almost in a similar manner as the temperature stratification behaviour, mass stratification can be observed inside the cavity with high concentration of the low density fluid (vapour) at the upper region of the cavity, while the higher density fluid (air) is in the lower region of the cavity. Also, the moisture concentration decreases with increasing temperature gradients and increase with a reduction in the Temperature, this behaviour could be significant in moisture management in an indoor environment. The mass and temperature stratification effects can affect the flow and heat transfer inside the cavity as evidence in the stream function fields comparability (shown in Figure 8) for the un-humidified and humidified cases (with a mass fraction of 0.04 kg/kg and 0.008 kg/kg) with two different temperature gradient cases of 20 °C and 60 °C respectively.

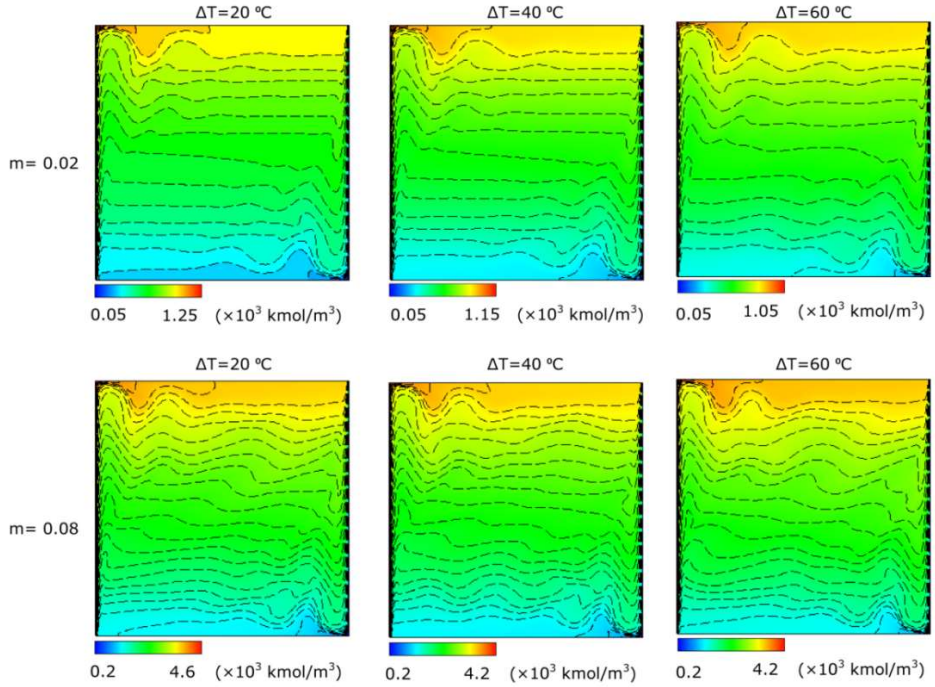

Figure 7: comparison of moisture concentration fields as a function of cavity vertical walls temperature gradient for two mass fraction of vapour.

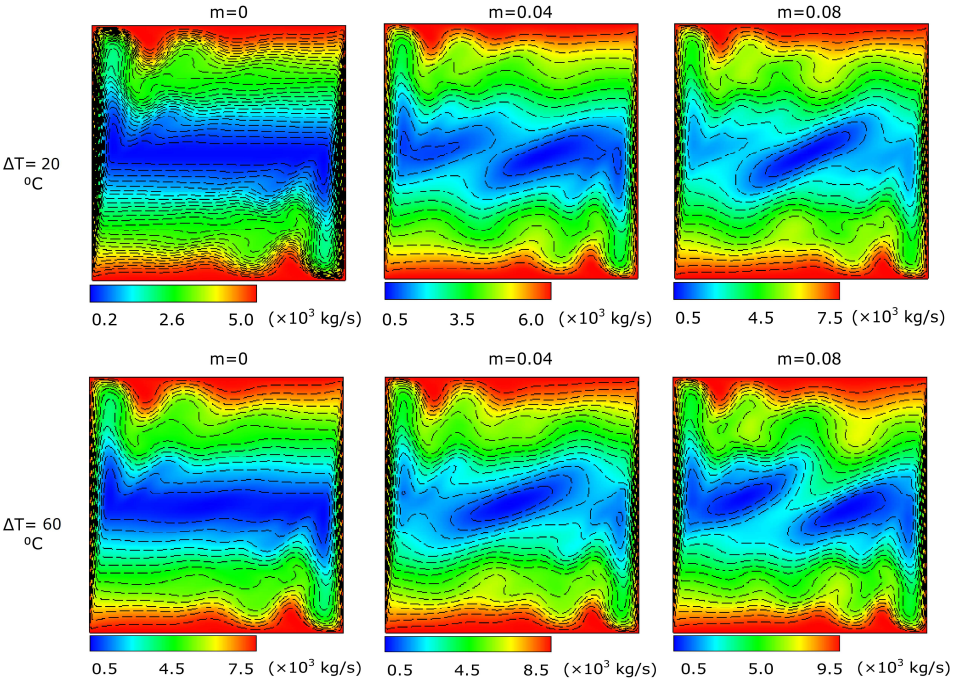

Figure 8: comparison of stream function fields as a function of vapour mass fraction for two temperature gradients of the cavity vertical walls.

5.3. The wall heat fluxes

The effects of moisture concentration on the natural convection heat transfer coefficient are presented in this section. The wall heat transfer coefficient results due to the variation of water vapour mass fraction with the vertical walls set at fixed

temperature gradient are presented first. This is followed by the case of varying the vertical wall temperature gradient at fixed water vapour mass fraction. The wall heat transfer coefficients were evaluated in terms of local Nusselt number and percentage change in average Nusselt number using Eq. (11) and Eq. (12) respectively.

The effect of moisture on the local Nusselt number profile along the cold and hot walls for various mass fractions of vapour with cavity vertical wall temperature gradients fixed at 40 °C is shown in Figure 9 (a) and (b) respectively. The heat transfer coefficient results for the un-humidify (m=0 kg/kg) cavity is also presented and was used as a bass case in order to estimate the influence of moisture variation on the heat transfer. The Nusselt number represents the heat transfer at the wall surface inside the cavity and is the ratio of convective to conductive heat transfer normal to the wall. The local and average Nusselt number is shown in Eq. (11) and Eq. (12) respectively.

$$Nu = \frac{Q_i L}{\bar{k}\left(T_h - T_c\right)} \tag{11}$$

$$\overline{Nu} = \frac{\bar{Q} L}{\bar{k}\left(T_h - T_c\right)} \tag{12}$$

Where $\bar{Q}$ is the integral average wall heat flux, L is the width of the cavity, $\bar{k}$ is the average fluid thermal conductivity and Q_i is the local heat flux evaluated at each node along a given wall.

The local Nusselt number profiles along the cold wall (Figure 9a) and the hot wall (Figure 9b) was compared for mass fraction values of water vapour ranging from 0 kg/kg to 0.1 kg/kg with an increment of 0.002 kg/kg in a 40 °C temperature gradient between the cavity vertical walls. It is observed that as the mass fraction of vapour increase the local Nusselt number along the wall also increase accordingly with an average increment of about 12.5% at the cold wall and 20.0 % at the hot wall. This was achieved by raising the mass fraction of the water vapour from 0 kg/kg to 0.1 kg/kg. On average, an increment of about 3.5% in the vertical walls local Nusselt number is achieved for every 0.002 kg/kg increment in the mass fraction of the water vapour, while the horizontal walls shows almost insignificant change in the local Nusselt number with a varying mass fraction of water vapour. This shows a significant increase in the heat transfer coefficient in the presence of moisture and the amount of moisture present in the air influence the magnitude of the heat transfer.

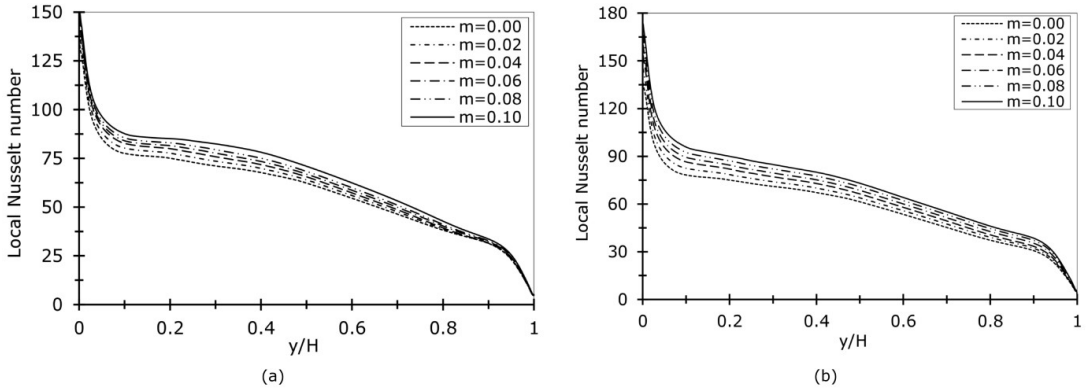

Figure 9: local Nusselt number comparison for various moisture concentrations, (a) cold wall (b) hot wall

The percentage change in the average Nusselt number is evaluated using Eq. (13). The percentage change of the average Nusselt number represents the percentage

change in the average Nusselt number between the humidified (moist-air) and the un-humidified (dry-air) conditions. Figure 10 (a-b) shows the comparison of the percentage change average Nusselt number as a function of mass fraction for different temperature gradients between the vertical walls. It is observed that the amount of moisture in the moist air has a significant effect on the heat transfer coefficient.

$$\% \ \Delta \overline{Nu} = \frac{\overline{Nu}_{wet} - \overline{Nu}_{dry}}{\overline{Nu}_{dry}} \times 100\% \tag{13}$$

The change in the average heat transfer coefficient as a function of the variation in the water-vapour content in moist air and the change in the vertical wall temperature gradient can be explained by the mass differential between dry air and water vapour. Since the molecular weight of water is less than that of dry air, an increase in the amount of water vapour in the moist air will increase the buoyancy force which will result in an increase in the convective current inside the cavity [51]. Hence, the species density gradient in the fluid mixture will increase with increasing water vapour content, which leads to the increase in the strength of convective current associated with natural convection flow inside the cavity.

Within the range of the temperature gradient between the vertical walls used in this study, the percentage change in average Nusselt number at the cold and hot walls increase proportionally with the increment in the mass fraction of water vapour as shown in Figure 10 (a-b). Generally, it is observed that the percentage change in average Nusselt number is almost directly proportional to the mass fraction of vapour present in the moist air and the gradient of the percentage change in average Nusselt number curve is optimum at lower temperature gradients than at higher temperature gradients.

Figure 10 (a-b) shows that for every 0.02 kg/kg increment in the mass fraction of water vapour there is about a 3.5% increase in the percentage change in average Nusselt number for the range of temperature gradient used in the study. For a mass fraction of 0.12 kg/kg at 20 °C temperature gradient between the vertical walls, an optimum value for the percentage change in average Nusselt number of about 27.5% and 34.8% is observed at the cold and hot wall as shown in Figure 10(a) and Figure 9 (b) respectively. For the temperature gradient of 40 °C at 0.12 kg/kg, the optimum percentage change in Nusselt numbers is about 13.5% and 24.5% at the cold and hot wall respectively. An optimum increment of about 8% and 18.5% in the percentage change in average Nusselt number is observed for a mass fraction of 0.12 kg/kg and temperature gradient of 60 °C at the cold and hot wall respectively. Therefore, depending on the temperature profiles between the vertical walls and the mass fraction of vapour the buoyancy-driven flow heat transfer coefficient could be affected significantly.

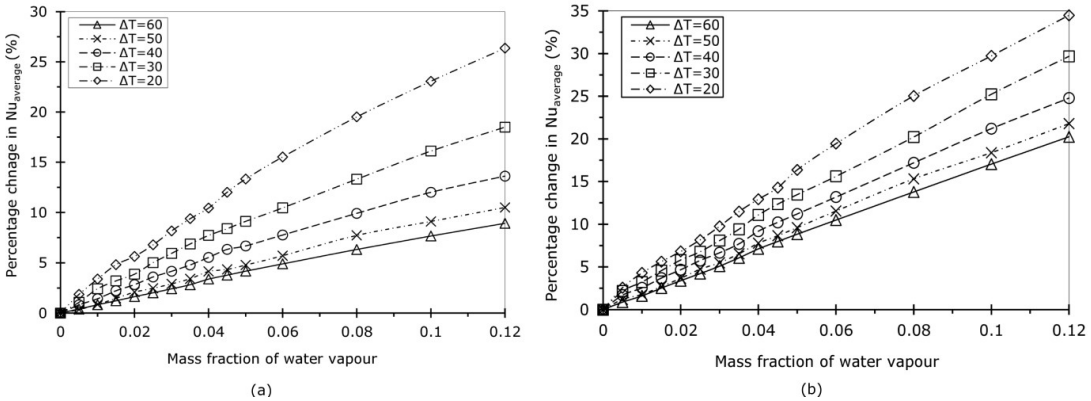

Figure 10: comparison of the percentage change in average Nusselt number as a function of vapour mass fraction for various vertical wall temperature gradients (a) cold wall (b) hot wall

The variation of the percentage change in average Nusselt number as a function of the temperature gradients between the vertical walls for various mass fractions of vapour have been compared for both cold and hot walls as in shown Figure 11(a) and (b) respectively. A range of practical mass fraction values of moisture within the indoor environment was used for the investigations as presented earlier in Figure 5. Most of the relative humidity thresholds are below 100%, except for the mass fraction of 0.04 and 0.035 kg/kg that gave a value slightly greater than the 100% thresholds at 20 °C temperature gradient.

It is our intension to quantify the effect of moisture concentration as a function of temperature on the heat transfer coefficient even before condensation occurs. As shown in Figure 11 (a-b) at both vertical walls. The percentage change in the average Nusselt number decreases with increasing temperature gradients within the range of mass fraction value used. This is of importance in the management of moisture so that the relative humidity remains below a given threshold. This could be achieved by identifying sensitive areas to lower/raise moisture content or increase/decrease temperature in order to avoid condensation in such enclosed system.

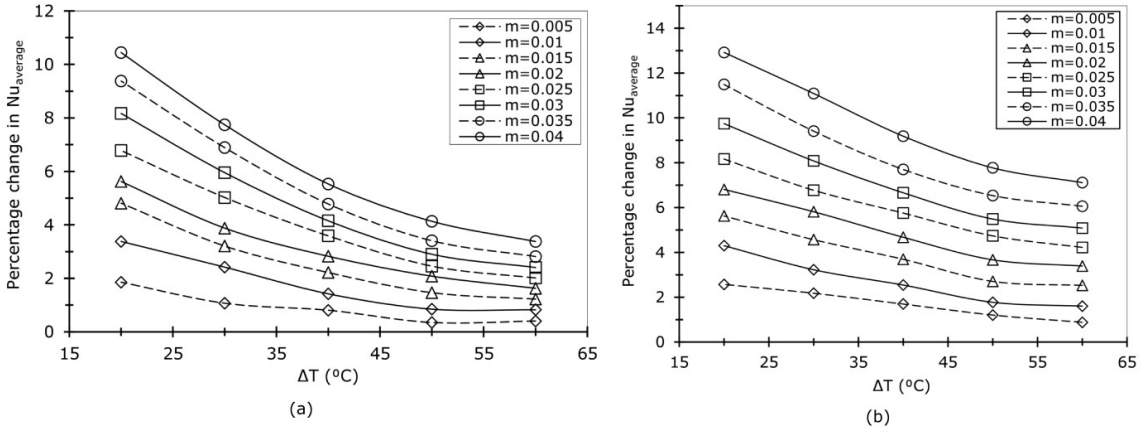

Figure 11: comparison of the percentage change in average Nusselt number as a function of vertical wall temperature gradients for various vapour mass fraction (a) cold wall (b) hot wall

6.0. **Conclusions**

The behaviour of buoyancy-driven flow distributions and heat transfer in a rectangular cavity due to variable moisture concentration as a function of temperature gradients between the vertical walls of the cavity was investigated and analysed numerically. Sensitivity analysis of the grid was conducted and the flow velocity, temperature and both the local and average Nusselt number results of the cavity filled with dry air compared favourably well against similar experimental benchmark study [8]. The effect of moisture was explored by varying the mass fraction of moisture at different temperature gradients between the vertical walls. The flow fields inside the cavity and the heat transfer coefficient for the various values of the mass fraction of vapour and temperature gradients has been compared and analysed accordingly. Key conclusions that can be drawn from the results are:

a) The presence of moisture causes changes in the energy equation, which has a significant effect on the heat transfer coefficient and influences the weak natural convection flows inside the cavity.
b) The percentage change in the average Nusselt number could be varied significantly depending on the moisture content and the vertical wall temperature gradients.

c) The percentage change in the average heat transfer coefficient increases by about 3.5% for every 0.02 kg/kg increment in their mass fraction of moisture within the range of temperature gradients used.
d) The vertical walls have been found to show greater sensitivity of the heat transfer with changes in moisture content, while both horizontal walls are almost insensitive to moisture content variation.
e) The heat transfer coefficient increases proportionally with increasing moisture concentration, while the average relative humidity inside the cavity significantly reduces with increasing temperature gradients between the vertical walls of the cavity. However, the percentage change in the average heat transfer coefficient decreases with increasing temperature gradient between the vertical walls.

This study has successfully shown that natural convection flow and heat transfer are very sensitive to moisture and its amount present in the air and even at low temperature gradient between the cavity vertical walls. The findings are of particular importance for the management of condensation in electronic enclosures and energy consumption in building space and storage operations. This could be achieved by designing such enclosure so that the relative humidity remains below a given threshold or by identifying sensitive areas that prone to high levels of moisture where the moisture content/temperature could be lower or raise in order to avoid condensation inside such enclosed system.

References

[1] M. Huang, P. Eames, B. Norton and N. Hewitt, "Natural convection in an internally finned phase change material heat sink for the thermal management of photovoltaics," *Solar Energy Materials and Solar Cells,* vol. 95, no. 7, pp. 1598-1603, 2011.

[2] E. Dascalaki, M. Santamouris, C. Balaras and D. Asimakopoulos, "Natural convection heat transfer coefficients from vertical and horizontal surfaces for building applications," *Energy and Buildings,* vol. 20, no. 3, pp. 243-249, 1994.

[3] S. Kadem, A. Lachemet, R. Younsi and D. Kocaefe, "3d-Transient modeling of heat and mass transfer during heat treatment of wood," *International Communications in Heat and Mass Transfer,* vol. 38, no. 6, pp. 717-722, 2011.

[4] H. Buchberg, I. Catton and D. K. Edwards, "Natural Convection in Enclosed Spaces—A Review of Application to Solar Energy Collection," *Journal of Heat Transfer,* vol. 98, no. 2, pp. 182-188, 2010 .

[5] W. Chen and W. Liu., "Numerical and experimental analysis of convection heat transfer in passive solar heating room with greenhouse and heat storage," *Solar Energy,* vol. 76, no. 5, pp. 623-633, 2004.

[6] C. S. Suvash and M. Khan, "A review of natural convection and heat transfer in attic-shaped space," *Energy and Buildings,* vol. 43, no. 10, pp. 2564-2571, 2011.

[7] H. Singh and E. C. Phili, "A review of natural convective heat transfer correlations in rectangular cross-section cavities and their potential applications to compound parabolic concentrating (CPC) solar collector cavities," *Applied Thermal Engineering,* vol. 31, no. 14, pp. 1359-4311, 2011.

[8] F. Ampofo and T. Karayiannis, "Experimental benchmark data for turbulent natural convection in an air filled square cavity," *International Journal of Heat and Mass Transfer,* vol. 46, no. 19, pp. 3551-3572, 2003.

[9] P. François, S. Olivier and S. Didier, "Preliminary experiments on the control of natural convection in differentially-heated cavities," *International Journal of Thermal*

Sciences, vol. 49, no. 10, pp. 1911-1919, 2010.

[10] A. A. Dafa'Alla and P. L. Betts, "Experimental Study of Turbulent Natural Convection in a Tall Air Cavity," *Experimental Heat Transfer: A Journal of Thermal Energy Generation, Transport, Storage, and Conversion,* vol. 9, no. 2, pp. 165-194, 1996.

[11] S. Didier, R. Nicolas, D. Francis and P. François, "Natural convection in an air-filled cavity: Experimental results at large Rayleigh numbers," *International Communications in Heat and Mass Transfer,* vol. 38, no. 6, pp. 679-687, 2011.

[12] G. McBain, "Natural convection with unsaturated humid air in vertical cavities," *International Journal of Heat and Mass Transfer,* vol. 40, no. 13, pp. 3005-3012, 1997.

[13] T. Catalin, H. Raluca, R. Gilles and W. Monika, "Numerical prediction of indoor air humidity and its effect on indoor environment," *Building and Environment,* vol. 38, no. 5, pp. 655-664, 2003.

[14] O. Laguerre, S. Benamara, D. Remy and D. Flick, "Experimental and numerical study of heat and moisture transfers by natural convection in a cavity filled with solid obstacles," *International Journal of Heat and Mass Transfer,* vol. 52, no. 25, pp. 5691-5700, 2009.

[15] H. Sun, G. Lauriat and X. Nicolas, "Natural convection and wall condensation or evaporation in humid air-filled cavities subjected to wall temperature variations," *International Journal of Thermal Sciences,* vol. 50, no. 5, pp. 663-679, 2011.

[16] Z. Hai-Xiang and M. Frédéric, "A review on the prediction of building energy consumption," *Renewable and Sustainable Energy Reviews,* vol. 16, no. 6, pp. 3586-3592, 2012.

[17] W. Monika, K. Targo, A. Marc Olivier, S. Marijke and S. K. Angela, "The effect of combining a relative-humidity-sensitive ventilation system with the moisture-buffering capacity of materials on indoor climate and energy efficiency of buildings," *Building and Environment,* vol. 44, no. 3, pp. 515-524, 2009.

[18] V. B. Marnix, S. Marijke, J. Arnold and D. P. Michel, "Heat, air and moisture transport modelling in ventilated cavity walls," *Journal of Building Physics,* vol. 38, no. 4, p. 317–349, 2015.

[19] E. Mathioulakis, V. Karathanos and V. Belessiotis, "Simulation of air movement in a dryer by computational fluid dynamics: application for the drying of fruits," *Journal of Food Engineering,* vol. 36, no. 2, pp. 183-200, 1998.

[20] P. Mirade and J. Daudin, "A numerical study of the airflow patterns in a sausage dryer," *Drying Technology,* vol. 18, no. 1-2, pp. 81-97, 2000.

[21] J. K. Atkinson, "Environmental conditions for the safeguarding of collections: A background to the current debate on the control of relative humidity and temperature," *Studies in Conservation: International Institute for Conservation of Historic and Artistic Works,* vol. 59, no. 4, pp. 205-212, 2014.

[22] F. Rawlins and G. Ian, "The control of temperature and humidity in relation to works of art," *Museums Journal,* vol. 41, pp. 279-283, 1942.

[23] Conservation, Association for Preservation Technology & American Institute for, "The New Orleans Charter for the Joint Preservation of Historic Structures and Artifacts," *APT Bulletin: The Journal of Preservation Technology,* vol. 27, no. 3, pp. 57-60, 1996.

[24] M. F. Mecklenburg, "Determining the Acceptable Ranges of Relative Humidity and Temperature in Museums and Galleries, Part 1, Structural Response to Relative Humidity," Museum Conservation Institute, 2007.

[25] L. Fang, G. Clausen and P. O. Fanger, "Temperature and humidity: important factors for perception of air quality and for ventilation requirements," *A S H R A E Transactions,* vol. 106, no. 2, pp. 503-510, 2000.

[26] T. Jørn, S. J. Anette and P. Fanger, "Upper limits for indoor air humidity to avoid uncomfortably humid skin," *Energy and Buildings,* vol. 28, no. 1, pp. 1-13, 1998.

[27] L. Jing, Y. Runming and M. Rachel, "An investigation of thermal comfort adaptation behaviour in office buildings in the UK," *Indoor and Built Environment,* vol. 23, no. 5, p. 675–691, 2014.

[28] T. Jørn, S. J. Anette and P. Fanger, "Upper limits of air humidity for preventing warm respiratory discomfort," *Energy and Buildings,* vol. 28, no. 1, pp. 15-23, 1998.

[29] O. Laguerre, D. Remy and D. Flick, "Airflow, heat and moisture transfers by natural convection in a refrigerating cavity," *Journal of Food Engineering,* vol. 91, no. 2, pp. 197-210, 2009.

[30] O. Laguerre, S. Benamara and D. Flick, "Numerical simulation of simultaneous heat and moisture transfer in a domestic refrigerator," *International Journal of Refrigeration,* vol. 33, no. 7, pp. 1425-1433, 2010.

[31] W. M. Yan and T. F. Lin, "Effects of wetted wall on natural convection heat transfer between vertical parallel plates," *Heat and Mass Transfer,* vol. 23, no. 5, p. 259–266, 1988.

[32] L. Yur-Tsai, H. Young-Ming and W. Chi-Chuan, "Performance of the herringbone wavy fin under dehumidifying conditions," *International Journal of Heat and Mass Transfer,* vol. 45, no. 25, pp. 5035-5044, 2002.

[33] H. Dol and K. Hanjalić, "Computational study of turbulent natural convection in a side-heated near-cubic enclosure at a high Rayleigh number," *International Journal of Heat and Mass Transfer,* vol. 44, no. 12, pp. 2323-2344, 2001.

[34] Y. Jaluria, Natural Convection Heat and Mass Transfer, Oxford: Pergamon Press, 1980.

[35] *ANSYS Academic Research Fluent, Release 14.0,* 2011.

[36] N. Tomás and S. Da-Wen, "Computational fluid dynamics (CFD) – an effective and efficient design and analysis tool for the food industry: A review," *Trends in Food Science & Technology,* vol. 17, no. 11, pp. 600-620, 2006.

[37] X. Bin and S. Da-Wen, "Applications of computational fluid dynamics in the food industry: a review," *Computers and Electronics in Agriculture,* vol. 34, no. 1, pp. 5-24, 2002.

[38] S. V. Patankar, Numerical Heat Transfer and Fluid Flow, Wood Dale, IL, U.S.A.: Taylor and Francis, 1980.

[39] J. H. Ferziger and M. Peric, Computational Methods for Fluid Dynamics., 3. Edition, Ed., Springer-Verlag, 2001.

[40] D. Qi-Hong and D. Guang-Fa Tang, "Special Treatment Of Pressure Correction Based On Continuity Conservation In A Pressure Based Algorithm," *Numerical Heat Transfer, Part B: Fundamentals: An International Journal of Computation and Methodology,* vol. 42, no. 1, pp. 73-92, 2002.

[41] B. Launder and D. B. Spalding, "The numerical computation of turbulent flows," *Computer Methods in Applied Mechanics and Engineering,* vol. 3, no. 2, pp. 269-289, 1974.

[42] R. Henkes and C. J. Hoogendoorn, "Comparison of turbulence models for the natural convection boundary layer along a heated vertical plate," *Int. J. Heat Mass Transfer,* vol. 32, pp. 157-169, 1989.

[43] V. C. Patel, W. Rodi and G. Scheuerer, "Turbulence models for near-wall and low Reynolds number flows - A review," *AIAA Journal,* vol. 23, no. 9, pp. 1308-1319, 1985.

[44] B. Launder and B. Sharma, "Application of the energy-dissipation of turbulence to calculation of low near a spinning disc," *Lett Heat Mass Transfer,* vol. 1, pp. 131-

138, 1974.

[45] J. H. Ferziger and M. Peric, Computational Methods for Fluid Dynamics, New York, USA: Springer, 2002.

[46] A. Mathur and S. He, "Performance and Implimentation of Launder-Sharma Low-Reynolds number Turbulence Model," *Computer and Fluids,* vol. 79, pp. 134-139, 2013.

[47] D. Iyi, R. Hasan and R. Penlington, "Interaction effects between surface radiation and double-diffusive turbulent natural convection in an enclosed cavity filled with solid obstacles," in *ICHMT International Symposium on Advances in Computational Heat Transfer*, Bath, England, 2012.

[48] S. Chandrasekhar, Radiative transfer, New York: Dover Publications, 1960.

[49] R. Siegel and J. Howell, Thermal radiation heat transfer, 4th ed., London: Taylor & Francis, 2002.

[50] H. K. Versteeg and W. Malalasekera, An Introduction to Computational Fluid Dynamics: The Finite Volume Method, 2nd ed., Essex: Pearson Education Limited, 2007.

[51] D. Iyi, R. Hasan and R. Penlington, "Effect of Emissivity on the Heat and Mass Transfer of Humid Air in a Cavity Filled with Solid Obstacles," *Numerical Heat Transfer, Part A: Applications - An International Journal of Computation and Methodology,* vol. 67, no. 5, pp. 531-546, 2014.